Selective hydrogenation of cinnamaldehyde in supercritical CO2 over Pt/SiO2 and Pt/HS-CeO2: An insight about the role of carbonyl interaction with supercritical CO2 or with ceria s...

ARTICLE *in* APPLIED CATALYSIS A GENERAL · OCTOBER 2013

Impact Factor: 3.94 · DOI: 10.1016/j.apcata.2013.07.028

4 AUTHORS, INCLUDING:

C.M. Piqueras
Universidad Nacional del Sur
14 PUBLICATIONS **117** CITATIONS
SEE PROFILE

Daniel A. Vega
Instituto de Física del Sur- IFISUR CONICET
78 PUBLICATIONS **647** CITATIONS
SEE PROFILE

Applied Catalysis A: General 467 (2013) 253–260

Contents lists available at ScienceDirect

Applied Catalysis A: General

journal homepage: www.elsevier.com/locate/apcata

Selective hydrogenation of cinnamaldehyde in supercritical CO_2 over Pt/SiO_2 and $Pt/HS\text{-}CeO_2$: An insight about the role of carbonyl interaction with supercritical CO_2 or with ceria support sites in cinamyl alcohol selectivity

Cristian M. Piqueras[a,*], Victoria Gutierrez[a], Daniel A. Vega[b,1], Maria A. Volpe[a]

[a] Planta Piloto de Ingeniería Química, PLAPIQUI-Universidad Nacional del Sur-CONICET, Camino La Carrindanga km 7-CC 717, 8000 Bahía Blanca, Argentina
[b] Instituto de Física del Sur, IFISUR-CONICET, Dep. Física-Universidad Nacional del Sur, Av. Alem 1253, 8000 Bahía Blanca, Argentina

ARTICLE INFO

Article history:
Received 26 April 2013
Received in revised form 1 July 2013
Accepted 14 July 2013
Available online 22 July 2013

Keywords:
Cinnamaldehyde
Supercritical carbon dioxide
Ceria
Selective hydrogenation

ABSTRACT

The catalytic hydrogenation of cinnamaldehyde employing H_2 as the reductant was carried out under supercritical (sc) CO_2, propane and other CO_2 dense mixture, employing Pt supported on silica and high surface (HS) ceria. The phase behavior of the mixtures was found to be in good agreement with the predictions obtained from the MHV2 (modified Huron-Vidal second-order) model. In order to study the influence of $scCO_2$ on the selectivity, the reaction was also conducted in dense propane and near-critical CO_2–isopropanol mixtures. These results were compared with those corresponding to classical gas–liquid conditions with isopropanol as solvent and low H_2 pressure. In $scCO_2$, the selectivity to cinnamyl alcohol over Pt/SiO_2 was 91%, quite higher than under classical conditions (38%). Such an enhancement is originated by the interaction of the C=O with $scCO_2$. For $Pt/HS\text{-}CeO_2$ the selectivity under supercritical conditions was slightly lower (80%) than the one corresponding to Pt/SiO_2 but quite higher than the one corresponding to gas–liquid conditions (54%). The interaction of the carbonyl group with ceria support predominates in this case, thus, the beneficial effect of $scCO_2$ is not observed in the same magnitude as in the case of Pt/SiO_2. A catalytic scenario is drawn for each catalyst in order to explain the different selectivity patterns.

1. Introduction

Many technological advantages arise when supercritical fluids (SCF) are employed as a reaction media in a wide variety of catalytic processes [1]. From the point of view of the Green Chemistry, the SCF method reduces dramatically the use of organic solvents, turning the process an environmentally friendly alternative [2]. In addition, if complete miscibility of reactants in SCF is accomplished, very high reaction rates and selectivities are attained [1]. Furthermore, subtle changes in the pressure and/or in the temperature lead to important variations in the physicochemical properties of the solvent (e.g. dipolar moment, density, viscosity, etc.) [3]. In this way, the solvent–substrate interaction can be tuned for improving the chemical reactivity of a specific functional group. Up to now, supercritical carbon dioxide ($scCO_2$) has been successfully employed in different catalytic reactions [4]. Examples include the selective hydrogenation of cinnamaldehyde over Pt supported on silica or alumina catalysts [5–7]. It was reported that the selectivity to cinnamyl alcohol was as high as 93% in $scCO_2$ [4], while over an identical unpromoted Pt catalysts in ethanol with 40 bar of H_2 the selectivities drastically dropped below 50% [8].

In order to obtain high selectivities over Pt based catalysts in gas–liquid conditions, two main routes in the formulation of the samples have been be followed: the addition of a promoter (Sn [9], Zn [10]) or the employment of reducible oxides [11,12]. The major advantage of $scCO_2$ application is the simplicity of the catalysts preparation, since no complex procedure seems to be required to achieve high yields. The insertion of CO_2 in the reaction media can produce strong modifications in the catalytic pattern, leading to "easy reactions", insensible to particle size [13,14].

High selectivities observed with $scCO_2$ have been explained based on different approaches: (i) from FTIR experiments, it was suggested that a supercritical solvent modifies the properties of the metal [15]; (ii) an interaction between $scCO_2$ and the organic molecules engaged in the reaction is developed which activates the carbonyl group [16]; (iii) an enlargement of the CO_2 quadrupole moment arises in the supercritical zone, increasing the Lewis acid–Lewis base (LA–LB) interaction between the solvent and

* Corresponding author. Tel.: +54 2914861700; fax: +54 2914871600.
E-mail addresses: cpiqueras@plapiqui.edu.ar, piqueras.martin@gmail.com (C.M. Piqueras).
[1] Tel.: +54 2914595100.

0926-860X/$ – see front matter © 2013 Elsevier B.V. All rights reserved.
http://dx.doi.org/10.1016/j.apcata.2013.07.028

the α–β compound [17,18]. This cooperative interaction between hydrogen from aldehyde and an oxygen atom from CO_2, weakens the carbonyl bond, giving rise to an enhanced activity of the C=O group hydrogenation against the C=C one.

In the present work, we study the nature of the change in selectivity response during the hydrogenation of cinnamaldehyde under CO_2–substrate interactions. In order to get an insight on the role of catalytic surface, two different Pt catalysts with similar surface area are tested: SiO_2 and CeO_2 supported ones. Silica is an inert oxide, while ceria contains both redox and acid-basic sites, which have been proven to strongly influence on the catalytic behavior for selective hydrogenation reactions [19]. In addition to $scCO_2$, dense propane and a near-critical CO_2–isopropanol mixture were employed as solvents, and the results are compared with those corresponding to $scCO_2$.

Finally, for the sake of comparison, both catalysts are tested under classical gas–liquid conditions and conclusions are drawn.

2. Experimental

2.1. Catalysts preparation and characterization

Platinum based samples were prepared employing SiO_2 (Davison Chemical) and high surface ceria (HS-CeO_2, Rhône Poulenc) as supports. The incipient wetness method was followed to obtain a 2 wt% metal loading. An aqueous solution of H_2PtCl_6 (5.5 mg/cm^3) was contacted with the supports at room temperature for 24 h. Finally, the solids were calcined at 773 K for 4 h under chromatographic air flow.

The catalysts were characterized by means of FTIR spectroscopy. A Nicolet 20 DXB FTIR spectrometer with 4 cm^{-1} resolution and 100 scans/spectrum was employed. 30–40 mg of catalyst were pressed in a 13 mm in diameter disk, which was put in a metal holder. Adsorption experiments were carried out in a stainless steel IR cell equipped with removable CaF_2 windows, at 10^{-6} Torr (attained with a turbomolecular vacuum pump). Firstly, the samples were cleaned by heating under 5 Torr of oxygen. For the case of Pt/SiO_2 the heating temperature was 673 K, while for Pt/HS-CeO_2 a higher temperature (755 K) was necessary for eliminating carbonates. Subsequently, the gas was switched to H_2 for 1 h. Finally the cell was evacuated and cooled down to room temperature. The IR experiments involve dosing CO (5.0 Torr) to the sample at room temperature for 3 min. A spectrum is taken upon evacuating the cell for 15–25 min. The cell is then sequentially heated and spectra are collected again for the sake of comparison at room temperature.

The reducibility of the catalysts was studied in a TPR home made apparatus. 40 mg of catalyst were calcined at 723 K. The temperature was increased linearly from 293 to 873 K at 10 K/min under 5% H_2/Ar flow at 20 cm^3/min. The hydrogen consumption was measured with a thermal conductivity detector. The response of the detector was calibrated by reducing a known amount of CuO. Following the TPR experiment, dynamic hydrogen chemisorption measurements were performed. The samples were cleaned under 20 cm^3/min flow of Ar at 903 K. Afterwards, the system was cooled down to ambient temperature an 0.25 cm^3 of a 0.5% H_2/Ar mixture were admitted to the TPR reactor by means of a ten ports sampling Valco valve. The hydrogen injections were repeated till saturation. The catalyst hydrogen uptake was calculated from the substraction of the saturation peak to the chemisorption one. The metallic area was calculated assuming a H/Pt ratio of the unity.

Platinum particle size was determined by TEM measurements, on a Jeol 100 CX2 (Tokyo, Japan) apparatus. One hundred metal particles were measured to determine the size distribution. The average diameter <d> of the crystals was calculated from: $\langle d\rangle = (\Sigma n_i d_i)/\Sigma n_i$, where n_i is the number of particles of a given size d_i.

X-ray diffraction (XRD) spectra were obtained ex situ using a Philips PW1710 BASED diffractometer equipped with a Cu-Kα radiation source, and a curved detector of graphite operated at 45 kV y 30 mA. Platinum crystallite sizes were calculated from the line full width at half maximum of the primary Pt peak using the Scherrer equation with the Warren's correction for instrumental line broadening. The Pt particle sizes, either the ones calculated from XRD results or those obtained from TEM characterization, were recalculated to metal dispersion, D (Pt_{sup}/Pt_{total}), following the relationship from Scholten et al. [20] (Eq. (1))

$$D = 10^{21}\,\frac{6 \cdot M \cdot \rho_{site}}{d \cdot \rho_{metal} \cdot N} \quad (1)$$

where M is the atomic weight (195.1 g/mol for Pt); ρ_{site} is the platinum surface density (12.5 Pt atoms/nm^2); d is the average particle size (nm); ρ_{metal} is the metal density (21.45 g/cm^3) and N is the Avogadro number.

The metal content was determined by atomic absorption spectrometry (AAS) in a spectrometer Instrumentation Laboratory 551, employing an air–acetylene burner and a platinum hollow lamp unit.

Specific surface areas were evaluated by the BET method, from N_2 isotherms at 77 K measured on a volumetric system Nova 1200e Quantachrome Instruments.

FTIR spectra of crotonaldehyde, butyl aldehyde and crotyl alcohol were obtained with a Nicolet 6700 spectrometer, following the procedure employed by Dandekar et al. [21]. Sample disks were prepared by mixing the support or catalyst powder with KBr. Before acquiring the FTIR spectra, a drop of the substrate was put in contact with the solid and then it was evacuated at 323 K for a short period of time. In each case, the spectra were contrasted against those corresponding to crotonaldehyde on KBr disks.

XPS analysis was performed on Multitechnique Specs equipment provided with a dual Mg/Al X-ray source and hemispherical analyzer PHOIBOS 150 used in fixed analyzer-transmission mode (FAT). The spectra were obtained with 30 eV pass energy and Mg anode operated at 200 W. The pressure during the measurements was less than 2.10^{-12} MPa (2.10^{-8} mbar).

The samples were ground, pressed, supported on the sample holder and reduced under a flow of H_2/Ar at 573 K during 10 min in the reaction chamber. Subsequently, the samples were evacuated to ultra high vacuum for at least 2 hours prior to the readings.

2.2. Catalytic test

2.2.1. Cinnamaldehyde hydrogenation in supercritical conditions

The experiments were performed in a high pressure cell (23 cm^3) provided with a sapphire window which allows the visual inspection. Three solvents were tested: CO_2, a CO_2/isopropanol mixture and propane. The loading procedure consisted of introducing 0.120 g of pre-reduced catalyst and 0.550 g of cinnamaldehyde into the cell. Afterwards, the system was purged for three times with 1 MPa of CO_2 at 293 K, and then filled with liquid CO_2 at 5.8 MPa and 293 K by means of a jacketed high pressure generator attached to a circulating bath which allows a temperature control in the range of ±0.2 K. Then, 6.0 MPa of H_2 at 293 K, were loaded, reaching a pressure of 11.4 MPa at 293 K and 21.2 MPa at 323 K. The molar fraction composition was 0.009/0.946/0.046 of cinnamaldehyde/CO_2/H_2, respectively. The composition was calculated by means of a thermodynamic model previously reported [22]. 1.255 g of isopropanol was added when the solvent mixture CO_2/isopropanol was used, 20.1 MPa were reached at 323 K. The composition in this case was 0.010/0.048/0.900/0.042 molar fraction of cinnamaldehyde/isopropanol/CO_2/H_2, respectively. The same procedure was followed for propane. Liquid propane was loaded, at 293 K and 0.87 MPa, filling the cell together

Table 1
Experimental condition for the hydrogenation of cinnamaldehyde under high pressure conditions and 323 K. Molar fractions estimated following the procedure described in Ref. [22].

Solvent	Aldehyde/catalyst (mass ratio)	Aldehyde/solvent/H_2 (molar fraction)	Cell pressure (MPa)
CO_2	4.6	0.009/0.946/0.046	21.2 ± 0.7
CO_2 + isopropanol	4.3	0.010/0.048/0.900/0.042	20.1 ± 0.5
Propane	6.1	0.01/0.896/0.094	12.6 ± 0.1

with 3.1 MPa of H_2. The pressure reached in this case was 4.9 MPa, at 293 K and 12.6 MPa at 323 K. The mixture composition was 0.01/0.896/0.094 cinnamaldehyde/propane/H_2, respectively. Single-phase was confirmed through naked eye observations. The experimental conditions are summed up in Table 1.

In a typical run, the catalyst to cinnamaldehyde ratio was maintained in the range of 4–6.5. The heating period involves 10 ± 1.5 min, and the reaction is stopped (following 120 min at the selected temperature) by quenching and carefully depressuring the cell. The liquid obtained after evacuation was recovered using 4 cm^3 of isopropanol and subsequently diluted in the same solvent to reach a concentration of 0.1 M, to perform the chromatography analysis. Following this procedure, the selectivity and conversion measurements give small deviations (±2% and ±1.5%, respectively).

2.2.2. Cinnamaldehyde hydrogenation in liquid phase

Before testing, 0.150 g of catalyst was reduced in H_2 flow at 573 K during 1 h. The sample was handled without exposure to air and was introduced into a 100 cm^3 Parr reactor. Care was taken to avoid any trace of oxygen. Afterwards, a 0.1 M cinnamaldehyde solution in isopropanol was loaded and the temperature was raised up to 333 or 373 K. The H_2 pressure was set at 1 MPa, while the stirring rate was fixed at 800 rpm. Once these experimental conditions have been reached, the reaction is considered to be started. The absence of diffusion limitation outside the catalyst particle is checked by varying the weights as well as the stirring rate in the range 0.1–0.3 g and 300–1000 rpm, respectively. In all the cases, the Weisz–Prater (WP) criterion was employed in order to check absence of internal mass transfer control [23].

3. Results

3.1. Phase equilibrium modeling

The phase equilibrium of these systems was calculated with the MHV2 model (SRK and Huron-Vidal second-order mixing rule) [24]. Pereda et al. [22] have shown that this model provides an accurate description of the liquid–liquid and liquid–vapor phase boundaries of the mixtures synthesized by Bhanage et al. [5]. We employed the set of critical properties and acentric factors of pure components calculated by Pereda et al. as well as the same phase equilibrium diagram to study our experimental systems. Fig. 1(a) shows a pressure vs CO_2 molar fraction graph showing the equilibrium boundaries of CO_2–cinnamaldehyde ($x = 0$) and the CO_2–cinnamyl alcohol ($x = 1$) binary systems, following MHV2 model. The compositions are given on a H_2-free molar basis. It is worth noting that, if an experimental point lies below the line, then phase split occurs and the mixture will be heterogeneous. One phase equilibrium data corresponding to Ref. [7] (stars) as well as our own experimental data (circles) are shown. It can be observed that the prediction of the model is acceptable, and that the experiments were conducted in single-phase conditions as was confirmed by naked eye observations. Fig. 1(b) presents a similar phase diagram for CO_2–isopropanol–cinnamaldehyde–H_2 ($x = 0$) and CO_2–isopropanol–cinnamyl alcohol–H_2 ($x = 1$) while Fig. 1(c) shows the result for the propane–cinnamaldehyde–H_2 and propane–cinnamyl alcohol–H_2 systems (both lead to similar curves). From these figures, it can be concluded that all experiments were conducted within single-phase conditions.

3.2. Catalysts characterization

Metal loading for both catalysts are similar and very close to the nominal value, which indicates that the wetness impregnation procedure was successful (see Table 2). BET surface areas for Pt/SiO_2 and Pt/HS-CeO_2 are quite similar to the corresponding to the bare support.

Fig. 2(a) and (b) shows the TEM micrographs corresponding to Pt/SiO_2 and Pt/HS-CeO_2, respectively. Average particle size of Pt/SiO_2 is 2.8 nm. In the case of the ceria catalyst, the poor contrast between the support and the metal does not allow to observe a large number of Pt crystals (see Fig. 2(b)). Consequently, no reliable particle size can be reported for the ceria supported sample. This limitation of high surface ceria was previously reported for gold catalysts supported on the same oxide [28].

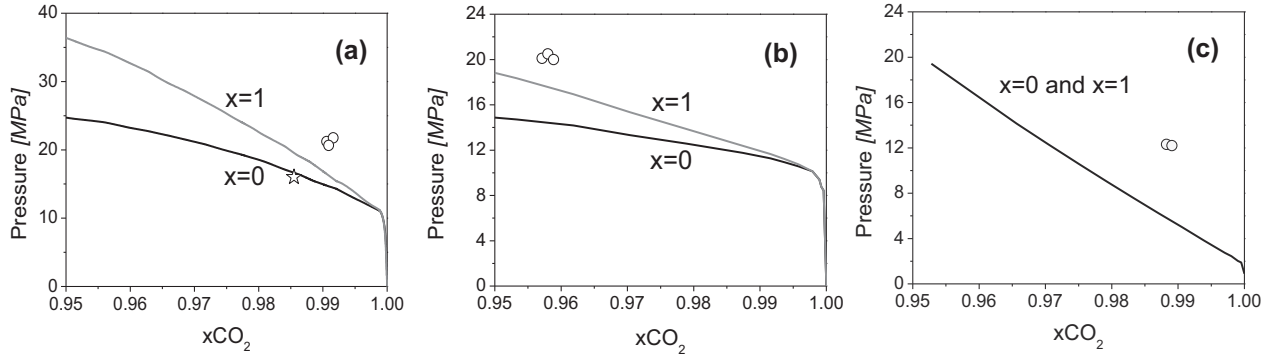

Fig. 1. H_2-free molar basis binary phase diagrams at high CO_2 mole fractions. MHV2 pressure predictions for: (a) CO_2–cinnamaldehyde ($x = 0$), CO_2–cinnamyl alcohol ($x = 1$), (b) binary systems (○) experimental data corresponding to the present work keeping constant the CO_2/H_2 and CO_2/isopropanol molar ratio equals to 21.43 and 18.75, respectively, (☆) from Ref. [7]. (b), CO_2–isopropanol–cinnamaldehyde–H_2 ($x = 0$) and CO_2–isopropanol–cinnamyl alcohol–H_2 ($x = 1$); (○) experimental data corresponding to the present work, constant CO_2/H_2 and CO_2/isopropanol molar ratio (21.43 and 18.75, respectively), (c) propane–cinnamaldehyde–H_2 and propane–cinnamyl alcohol–H_2 (○) experimental data corresponding to the present work, propane/H_2 mole ratio was 9.53.

Table 2
Catalytic properties of Pt/SiO_2 and $Pt/HS\text{-}CeO_2$ catalysts.

Catalyst	Surface area (m^2/g)	Part. size (nm)		Metal disp. (%)		H_2/Pt[b]	BE (eV)5/2	Pt 4f7/2
		TEM	XRD	XRD[a]	H_{2Chem} [c]			
Pt/SiO_2	260	2.8	3.1	36	41	0.99	73.5	70.5
$Pt/HS\text{-}CeO_2$	240	–	4.6	25	81	9.21	74.1	70.1

[a] Metallic dispersion as calculated from Scholten relationship [20] considering particle size from XRD.
[b] Molar ratio from TPR.
[c] Metallic dispersion obtained from H_2 chemisorption.

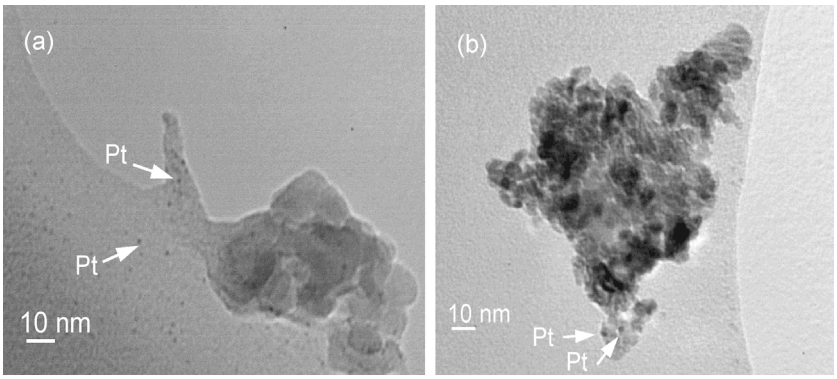

Fig. 2. TEM images of Pt/SiO_2 (a) and $Pt/HS\text{-}CeO_2$ (b) catalysts.

The FTIR spectra of adsorbed CO corresponding to both catalysts are shown in Fig. 3(a) and (b). For the platinum silica sample, two bands are observed, one at 2070 cm^{-1}, which is assigned to linear CO bonded to Pt^0 and other broad band with a maximum at 1819 cm^{-1} due to highly coordinated CO. These bands remain even after evacuating the system, indicating a strong CO–Pt interaction. The high area ratio between the bands associated to linear CO respect to the multiple coordinated one, indicates that the metal is highly dispersed. These results agree with the relatively small particle size determined by TEM images.

In the case of $Pt/HS\text{-}CeO_2$ much more bands than over Pt/SiO_2 are observed. It is important to establish that for platinum, no other species than Pt^0 are present in the ceria supported sample, as determined by XPS (this characterization will be discussed further). The one assigned to linear CO appears at 2080 cm^{-1}, while bands associated with a multiple coordination of CO are observed at 1965 and 1847 cm^{-1} [24] (see Fig. 3(b)). The area ratio between the bands associated to linear and multiple coordinated CO species is lower than that observed in Pt/SiO_2, which indicates an increment in the content of developed planes and a lower dispersion of the metal on ceria support.

Regarding the linear CO band, it is shifted to higher frequency by comparison with the band observed in the silica supported sample. Besides, a tail appears in the low frequency side. A commercial software allows the deconvolution and subtraction of the two overlapping bands: the first one centered at 2082 cm^{-1} (assigned to on-top adsorption of CO on platinum) and the second one at 2045 cm^{-1} (assigned to on-top adsorption of CO on platinum in strong interaction with Ce^{3+} centers [25,26]). Another broad band at 1730 cm^{-1} is detected, which is associated to a tilted specie, $Pt–CO–Ce^{3+}$, where both C and O are coordinated to the surface [24,26]. The bands at 2045 and 1730 cm^{-1} indicate the presence of interfacial metal-support sites, involving Ce^{3+}. It is important to emphasize that, in order to acquire the FTIR spectrum of the $Pt/HS\text{-}CeO_2$ catalyst, high dilution with KBr was carried out (10 mg of catalyst in 100 mg of KBr), leading to a low absorbance. The dilution is necessary since following the pre-reduction treatment, the samples become black and strongly reduce the light transmission. The dark coloration is attributed to the formation of substoichiometric ceria oxides (Ce^{3+} coexisting with Ce^{4+}) [27]. This feature was previously reported [28]. High quality CO signal in the FTIR spectrum has been reported for a 1 wt% $Pt/HS\text{-}CeO_2$ sample, however the support area was much lower (60 m^2/g)[26] than in the present study. In this case, $Pt–Ce^{3+}$ interaction were detected after an intense pre-reduction step (573 K in H_2 atmosphere during 12 h).

Summing up, the FTIR characterization of CO adsorbed onto $Pt/HS\text{-}CeO_2$ and on Pt/SiO_2 indicates that a strong interaction

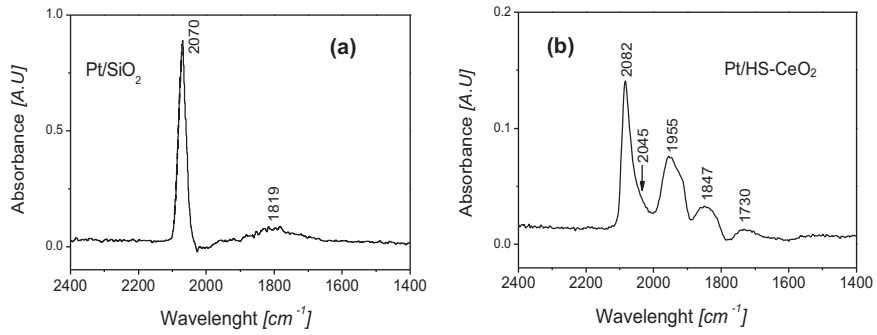

Fig. 3. FTIR spectra of CO adsorption onto $Pt/HS\text{-}CeO_2$ (a) and Pt/SiO_2 (b) catalysts.

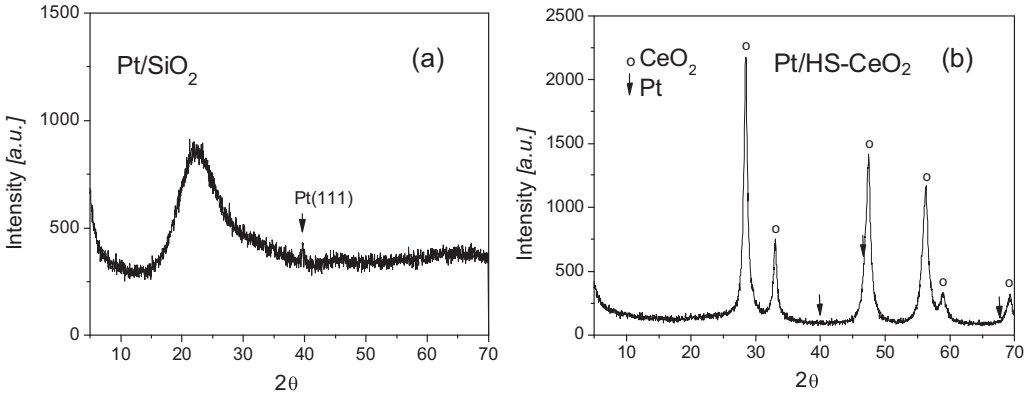

Fig. 4. XRD spectra of Pt/SiO_2 (a) and $Pt/HS\text{-}CeO_2$ (b) catalysts.

between the metal and the support arises for the former catalyst. Besides it is concluded that Ce^{3+} species influence on the adsorption of CO.

Particles sizes and metallic dispersion are reported in Table 2. The dispersion values were calculated from XRD (Fig. 4(a) and (b)) as well as from H_2 chemisorptions tests, considering hemispheric shapes (see Table 2). From XRD, the metallic dispersion for $Pt/HS\text{-}CeO_2$ is lower than for Pt/SiO_2, which is in agreement with the FTIR results. The metallic dispersion obtained from H_2 chemisorption of Pt/SiO_2 is in good agreement with that calculated from XRD. On the contrary, for $Pt/HS\text{-}CeO_2$, the value obtained from H_2 chemisorption is three times higher than that calculated from XRD. Such a high hydrogen uptake leads to a huge metal dispersion (81%) and is not in line with the FTIR results for $Pt/HS\text{-}CeO_2$. Thus, the extra amount of hydrogen uptake would be related with Ce^{3+} sites located at the Pt–ceria interface which are able to absorb hydrogen [29]. This result shows that ceria surface can activate H_2, and that it would provide reactive sites for the hydrogenation.

The TPR profiles of the catalysts are shown in Fig. 5. For the silica sample a broad consumption peak appears at 423 K. The amount of H_2 consumed corresponds to the complete reduction of platinum, giving rise to an H/Pt ratio close to one (see Table 2). In the case of $Pt/HAS\text{-}CeO_2$, a narrow peak is observed at 413 K. The H_2 consumption largely exceeds the one corresponding to the complete reduction of PtO_2 (H_2/Pt ratio equals 9.2), indicating that the support is also being reduced. Considering that such a reduction is depicted by the reaction $2CeO_2 + H_2 \rightarrow Ce_2O_3 + H_2O$, the additional engages 16.4% of ceria. This result evidences a relatively high concentration of Ce^{3+} available in the catalytic surface.

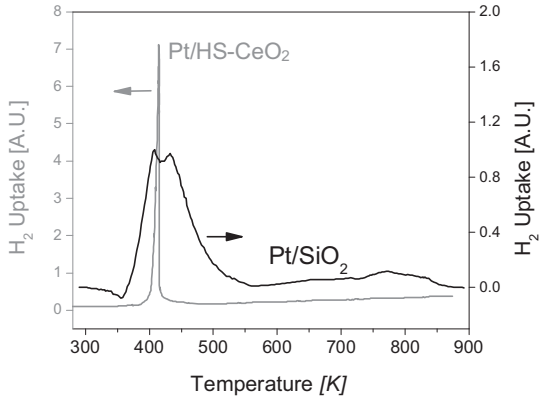

Fig. 5. Hydrogen consumption of Pt/SiO_2 (a) and $Pt/HS\text{-}CeO_2$ (b) catalysts in the TPR measurements.

For bare $HS\text{-}CeO_2$, the reduction of the surface Ce^{4+} species is accomplished between 573 and 773 K [19]. From the TPR results, it is evident that this process in markedly enhanced due to the presence of the metal, which dissociates H_2 at a relatively low temperature. The enhanced reduction of support species was previously observed for gold supported on $HS\text{-}CeO_2$ [19] and onto iron oxides [30]. It is likely that it occurs also in the metal-support boundary [28].

The XPS characterization of the sample was carried out in order to investigate on the chemical state of platinum in Pt/SiO_2 and in $Pt/HS\text{-}CeO_2$. Before analyzing the XPS result it should be considered that the catalysts of this study posses a large surface area (260 and 240 m^2/g) and a relative low metal loading, which turns the study rather difficult, as was already observed [19]. Besides, samples show significant charging, making the peaks extremely wide, with bad definitions. The XPS spectra of supported Pt in published works show relatively high quality results, however the metal loading in those works is relatively high (5%) and the specific surface area of the supports is generally lower than 100 m^2/g [31].

With this consideration in mind, Fig. 6 shows the binding energy (BE) of Pt 4f. The corresponding results are reported in Table 2. The

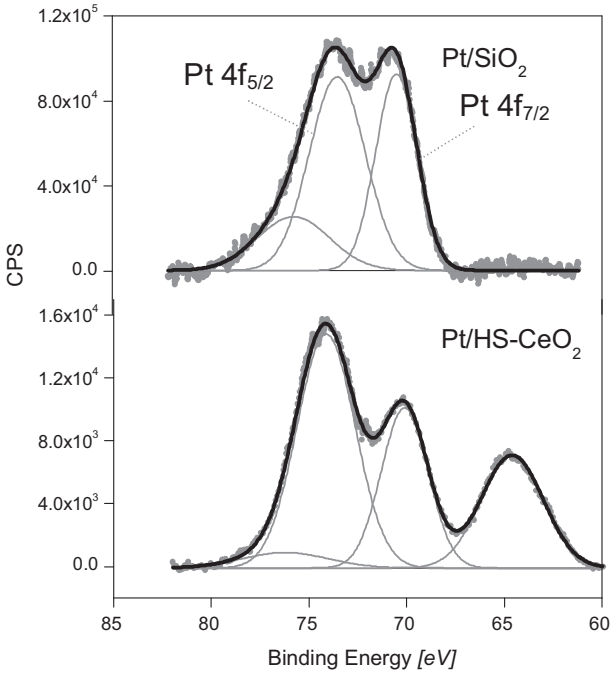

Fig. 6. XPS spectra of Pt 4f energy binding region of Pt/SiO_2 and $Pt/HS\text{-}CeO_2$ catalysts.

BE values suggest that platinum is in the 0 oxidation state for both samples, and that no electronic modifications of the metal occur.

3.3. Catalytic tests

3.3.1. Hydrogenation of cinnamaldehyde under liquid phase conditions

Table 3 reports the turn over frequencies (TOF), conversion and selectivity to cinnamyl alcohol achieved after 120 min. For gas–liquid conditions very low conversions were obtained by both catalysts at 333 K. In order to enlarge this level of conversion, the mass of catalyst should be increased to 600–800 mg, leading to high mass/reactant ratios. This procedure originates mass diffusion limitations, catalyst attrition and turns difficult the withdrawing of aliquots of the reactive mixture.

At 333 K and 7.5% of conversion, TOF values are similar for both catalysts, while at 373 K, and 15% of conversion, TOF number of the ceria supported sample is two fold higher than the TOF of the silica supported catalyst. The high activity of Pt/HS-CeO_2 can be attributed to a promotional effect of Ce^{3+} [32], which contributes with new active hydrogenating sites.

The selectivity toward cinnamyl alcohol measured over Pt/HS-CeO_2 is quite larger (50%) than that of Pt/SiO_2 (30%) in the 15% range of conversions (see Table 3). The high selectivity measured over ceria supported sample would be originated in an activation of the C=O bond on support sites, giving rise to an increase of the hydrogenation of the carbonyl bond against the olefinic one [28].

3.3.2. Hydrogenation of cinnamaldehyde under supercritical conditions

The hydrogenation of cinnamaldehyde was performed at 323 K, where the solubility of the aldehyde and the cinnamyl alcohol is higher in propane than in CO_2, as is evidenced by the lower pressure needed to reach a single-phase condition for the former solvent. A 8 MPa of CO_2 extra pressure is required to reach solubility to a similar mole fraction.

Table 3 summed up the results for the hydrogenation of cinnamaldehyde over Pt/HS-CeO_2 and Pt/SiO_2 employing different solvents (CO_2, a mixture of CO_2 and isopropanol and propane).

TOF values measured in the present work are similar to those obtained by Bhanage et al. (0.06 s^{-1}) for the same reaction in $scCO_2$ using 1 wt% Pt/Al_2O_3 catalyst [5].

Under $scCO_2$, both catalysts, Pt/SiO_2 and Pt/HS-CeO_2, have much higher activity than in gas–liquid conditions using isopropanol. This trend was also observed for the other sc solvents, as can be expected based on the advantage of supercritical media for increasing the mass transport, due to the low viscosity of the solvent (0.061 vs 1.062 cP, $scCO_2$ and isopropanol respectively [34]).

For the case of Pt/SiO_2 employing $scCO_2$, the selectivity is greatly increased by comparison with the classical gas–liquid conditions. This result is in agreement with previous reports, where it was found that the increase of selectivity is due to the enlargement of the dielectric constant of CO_2 in sc conditions [5].

The addition of isopropanol increases the value of the critical temperature of the mixture, from 291.5 K up to 305.2 K (calculated following reference [22]). Thus, at the reaction temperature (323 K), the advantageous properties of supercritical media are not lost. However, the incorporation of isopropanol leads to a notable diminution of the selectivity (see Table 3), indicating that the enhanced selectivity is associated to a solvent effect. The same conclusion was drawn by Meng et al., for the hydrogenation of chloronitrobenzene in $scCO_2$ [33]. These authors measured selectivities to chloroaniline and to aniline over Ni/TiO_2 in the range of 97–99.5%, which cannot be achieved over the same catalyst in ethanol or *n*-hexane solvents.

The above comment solvent effect suggests that the enhanced activation of C=O is due to $scCO_2$. The nature of such an effect could be explained by different approaches. It was suggested that a quadrupole/dipole interaction occurs between the solvent and the carbonyl group [35], due to the enlargement of the quadrupole moment of CO_2 in the supercritical region. It was also proposed, that one of the CO_2 oxygen atoms participates in a cooperative hydrogen bond with the electron-deficient hydrogen bond to the C of the carbonyl group (C—H···O) or to the R-carbon of the chain [36]. Wang et al. measured a red shift of about 40 cm^{-1} for C=O vibration in $scCO_2$ mixtures, attributing this bond enlargement to the interaction of cinnamaldehyde with four CO_2 molecules [37]. In our experiments, isopropanol dilutes the interaction of $scCO_2$ with the aldehyde reducing its beneficial effect. In order to prove that selectivity is related to the polar interaction with the solvent, we performed the hydrogenation with a nonpolar solvent (propane). The result is reported in Table 3 for the Pt/SiO_2 catalyst. In this case, the reaction conditions are away from the critical temperature of the mixture (375.2 K), and its properties are related to an expanded liquid (compressibility factor $Z = 0.4276$ and density equal to 434.3 kg/m^3) and not to a supercritical solvent. As in the previous case, the activity is higher than the obtained under liquid isopropanol, which could be attributed to the improvement of the mass transfer (the propane mixture and isopropanol viscosity are 0.086 vs 1.062 cP, respectively) [34]. On the contrary, the selectivity to cinnamyl alcohol is relatively low (36%), and no improvement against the reaction under classical conditions is observed. This result stresses the fact that the nature of the supercritical media is of paramount importance for developing a high selectivity.

Focusing the attention on the results of Pt/HS-CeO_2 under $scCO_2$, a similar enhancement of activity in comparison with the gas–liquid conditions is observed. Although high selectivity was measured for Pt/HS-CeO_2 (approximately 80%), this catalyst is less active and selective than Pt/SiO_2 tested in $scCO_2$. This is a quite surprising result, opposite to that observed for classical conditions. Table 3 shows that, when isopropanol is added to $scCO_2$, the selectivity measured over Pt/HS-CeO_2 is not depleted as occurs in the case of Pt/SiO_2. Thus, the source of the improvement (the solvent interaction with $scCO_2$) would be partially lost for the ceria catalyst. This effect could be attributed to the particular nature of HS-CeO_2 surface, possessing redox, basic and acidic sites, that strongly interacts with carbonyl of the substrate [32]. This support interaction would prevail over the solvent effect in the chemical reaction scenario.

To go further in the explanation of the different catalytic pattern commented above we investigated on the interaction the carbonyl group with the catalytic surface of Pt/HS-CeO_2 and Pt/SiO_2, FTIR spectra of crotonaldehyde adsorbed on HS-CeO_2 and SiO_2 bare supports as well as onto their corresponding Pt catalysts were taken. We have selected crotonaldehyde as model α,β-aldehyde, due to its more simple structure as compared with cinnamaldehyde. The assignment of the bands was performed based on previous works [21,38] and based on the analysis of FTIR spectra of crotyl alcohol and butanal adsorbed on SiO_2 and CeO_2.

Fig. 7(a) shows the spectra of crotonaldehyde in contact with HS-CeO_2 and with SiO_2. Silica clearly shows a different vibrations pattern than ceria. The bands at 1700 and 1723 cm^{-1} (SiO_2) and 1691 and 1722 cm^{-1} (HS-CeO_2) are assigned to C=O stretching, while the bands at 1662 and 1658 cm^{-1} are due to C=C olefinic stretching over silica and ceria respectively. Besides, the bands appearing at 1640 and 1641 cm^{-1} are assigned to the bending mode of water. Since all the above mentioned bands are related with the reactive groups, C=O and C=C, we will focus on this region.

When the bare supports are compared, the main difference is the relative intensity between the bands assigned to C=O and C=C stretching. While for SiO_2 the former bands are relatively more

Table 3
Selectivity and activity of Pt/SiO_2 and $Pt/HS\text{-}CeO_2$ in the hydrogenation of cinnamldehyde using $scCO_2$, propane and CO_2 + isopropanol mixture as well as in classical gas–liquid and low H_2 pressure.

Catalyst	T (K)	Solvent	X (%)	S (%)[d]	TOF[e] (s^{-1}) ($\times 10^3$)
Pt/SiO_2	333	Isoprop.	8.6[a]	38.0	3.3
	373	Isoprop.	16.5[b]	30.3	22.5
Pt/HS-CeO_2	333	Isoprop.	7.2[a]	54.3	4.1
	373	Isoprop.	14.4[b]	50.8	50.2
Pt/SiO_2 [c]	323	CO_2	12.5	91.3	10.3
Pt/SiO_2 [c]	323	CO_2 + isoprop.	18.7	52.7	16.8
Pt/SiO_2 [c]	323	Propane	21.7	36.5	17.0
$Pt/HS\text{-}CeO_2$ [c]	323	CO_2	10.3	80.3	8.9
$Pt/HS\text{-}CeO_2$ [c]	323	CO_2 + isoprop.	8.9	83.5	7.2

[a] Liquid phase, at 120 min of reaction time.
[b] Liquid phase, at 30 min of reaction time.
[c] Supercritical conditions, at 120 min of reaction time.
[d] Selectivity to cinamyl alcohol.
[e] Moles of cinnamaldehyde converted per second and per mole of exposed Pt.

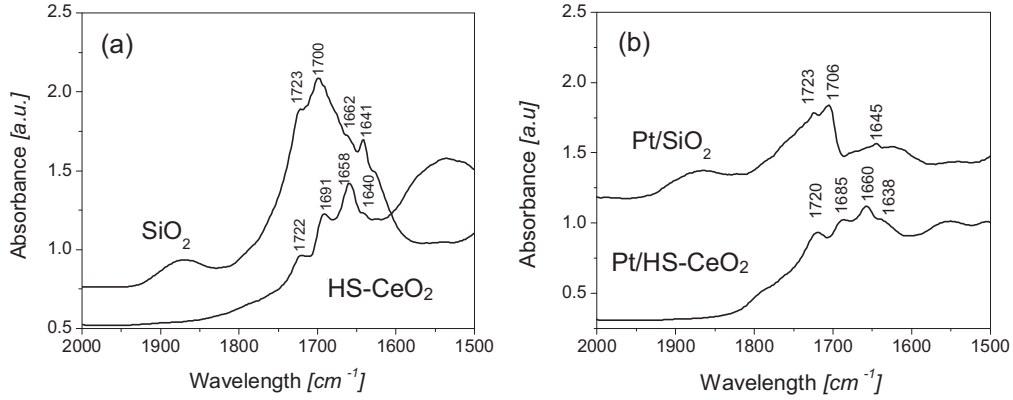

Fig. 7. FTIR spectra of crotonaldehyde adsorption on: (a) $HS\text{-}CeO_2$ and SiO_2, (b) $Pt/HS\text{-}CeO_2$ and Pt/SiO_2 catalysts.

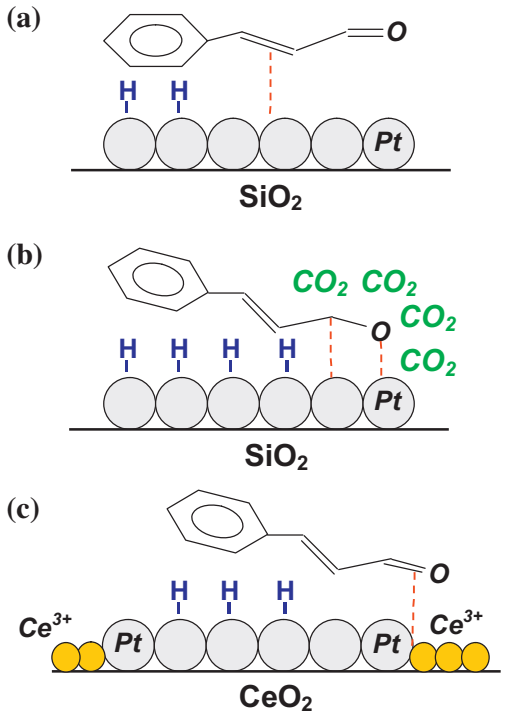

Fig. 8. Suggested scenario for cinnamaldehyde adsorption on: (a) Pt/SiO_2 under near critical CO_2 + isopropanol and gas–liquid conditions, (b) Pt/SiO_2 under $scCO_2$ and (c) $Pt/HS\text{-}CeO_2$ under both: gas–liquid and $scCO_2$.

intense than the ones due to C=C, for $HS\text{-}CeO_2$ the opposite trend was observed. From this comparison it could be concluded that the carbonyl group is more strongly bonded to ceria surface than to silica.

The same conclusion could be drawn for the case of the Pt catalysts, though the trends are more clearly observed (Fig. 7 (b)). The C=C band vanished from the spectrum of the silica supported catalyst. The band at 1685 cm^{-1}, due to C=O adsorbed on $Pt/HS\text{-}CeO_2$, is blue shifted (21 cm^{-1}) by comparison with the same band corresponding to Pt/SiO_2, indicating that the carbonyl bond is weaker in the former case. This difference would be originated in a strong interaction of carbonyl group with $HS\text{-}CeO_2$ sites, probably located at the Pt–ceria interface [32]. On the other hand, the band due to C=C remains unaffected.

From this FTIR analysis it is clear that a different interaction between the unsaturated aldehyde and the ceria or the silica surfaces is developed. Considering the above commented XPS results, ceria does not alter the chemical state of platinum, the interaction of the reactive species would be connected with ceria sites, more specifically Ce^{3+} centers. This interaction leads to an activation of the carbonyl group by comparison to the olefinic one in cinnamaldehyde and explains the larger selectivity of $Pt/HS\text{-}CeO_2$ measured under gas–liquid conditions.

The C=O–ceria interaction is also developed under supercritical conditions with a major effect due to the improvement of mass transference. In this way, the adsorption of carbonyl on the sites of the support could mask the beneficial effect of $scCO_2$.

This explains the catalytic result obtained when $scCO_2$ is diluted with isopropanol: over $Pt/HS\text{-}CeO_2$ the aldehyde–$scCO_2$ interaction

seems to be lost, since the dilution causes no effect on the activation of the carbonyl group.

For Pt/HS-CeO_2, the C=O–ceria interaction would be developed at the Pt–ceria interface, where Ce^{3+} species are present [32]. Furthermore, over these sites the H_2 dissociation would occur [28]. $scCO_2$ does not change this scenario and thus, no direct effect onto the surface chemistry is observed.

In Fig. 8, the models suggested for the different catalyst surfaces under gas–liquid or under supercritical conditions are shown. In model (a) the classic "π" adsorption intermediate is shown. This way of adsorption favors the hydrogenation of the olefinic bond, leading to a non selective catalytic behavior (Pt/SiO_2 with isopropanol or with CO_2 + isopropanol mixture). The model (b) represents the interaction of the α,β aldehyde with $scCO_2$, where the solvent turns the C=O bond weaker, favoring its adsorption and subsequent hydrogenation (Pt/SiO_2 with $scCO_2$). In the model (c), the sites of the support activate the C=O adsorption, as well as the dissociation of H_2, favoring the selectivity to cinnamyl alcohol (Pt/HS-CeO_2 either under gas–liquid or under supercritical conditions).

These observations provide clear evidence about the complex scenario presented by this reactants–catalysts system. Thus, it is hoped that this work will stimulate additional experimental and theoretical research to study the complex mechanism of interactions associated to this system.

4. Conclusions

The selective hydrogenation of cinamaldehyde to cinnamyl alcohol was achieved over Pt/SiO_2 in $scCO_2$ at a relatively low temperature (323 K). The supercritical CO_2 increases both, the activity and the desired selectivity, while nonpolar propane presents only a beneficial effect on activity.

The enlargement of the selectivity is originated by the interaction between $scCO_2$ and the α,β aldehyde, which turns more labile the C=O bond, thus increasing the rate of hydrogenation of carbonyl bond against the olefinic one. The beneficial effect of $scCO_2$ is partially reduced if an interaction between the aldehyde and active sites of the support arises, as in the case of Pt catalyst based on ceria of high surface area. In this case, the selectivity to cinnamyl alcohol does not depend on the supercritical solvent nature.

Acknowledgements

The authors would like to thanks to Dr. Ignacio Costilla by FTIR of adsorbed CO measurements. Also the authors would like to thanks to Agencia Nacional de Promoción Científica y Tecnológica, Ministerio de Ciencia, Tecnología e Innovación Productiva of Argentina fund code PICT 1353, Universidad Nacional del Sur and to Consejo Nacional de Investigaciones Científicas y Técnicas (CONICET) for the financial support for this work. Thanks are given to ANPCyT for the purchase of the SPECS multitechnique analysis instrument (PME8-2003).

References

[1] A. Baiker, Chem. Rev. 99 (1999) 453–473.
[2] M. Hitzler, F. Smail, S. Ross, M. Poliakoff, Org. Process Res. Dev. 2 (1998) 137–146.
[3] G. Jenzer, M. Schneider, R. Wandeler, T. Mallat, A. Baiker, J. Catal. 199 (2001) 141–148.
[4] M. Burk, S. Feng, M. Gross, W. Tumas, J. Am. Chem. Soc. 117 (1998) 8277–8278.
[5] B.M. Bhanage, Y. Ikushima, M. Shirai, M. Arai, Catal. Lett. 62 (1999) 175–177.
[6] F. Zhao, Y. Ikushima, M. Shirai, T. Ebina, M. Arai, J. Mol. Catal. A: Chem. 180 (2002) 259–265.
[7] M. Chatterjee, F.Y. Zhao, Y. Ikushima, Appl. Catal. A: Gen. 262 (2004) 93–100.
[8] M. Arai, H. Takahashi, M. Shirai, Y. Nishiyama, T. Ebina, Appl. Catal. A: Gen. 176 (1999) 229–237.
[9] F. Coloma, A. Sepúlveda-Escribano, J. Fierro, F. Rodriguez-Reinoso, Appl. Catal. A: Gen. 148 (1996) 63–80.
[10] S. Galvagno, Z. Poltarzewski, A. Donato, G. Neri, R. Pietropaolo, J. Mol. Catal. 35 (1986) 365–375.
[11] B. Campo, M. Volpe, C. Gigola, Ind. Eng. Chem. Res. 48 (2009) 10234–10239.
[12] M. Aramendía, V. Borau, C. Jiménez, J. Marinas, A. Porras, F. Urbano, J. Catal. 172 (1997) 46–54.
[13] F. Zhao, Y. Ikushima, M. Arai, J. Catal. 224 (2000) 479–483.
[14] F. Zhao, R. Zhang, M. Chatterjee, Y. Ikushima, M. Arai, Adv. Synth. Catal. 346 (2004) 661–668.
[15] M. Arai, Y. Nishiyama, Y. Ikushima, J. Supercrit. Fluids 13 (1998) 149–153.
[16] Y. Akiyama, S. Fujita, H. Senboku, C.M. Rayner, S.A. Brough, M. Arai, J. Supercrit. Fluids 46 (2008) 197–205.
[17] M.A. Blatchford, P. Raveendran, S.L. Wallen, J. Phys. Chem. A 107 (2003) 10311–10323.
[18] F. Zhao, S.-I. Fujita, S. Akihara, M. Arai, J. Phys. Chem. A 109 (2005) 4419–4424.
[19] B. Campo, S. Ivananova, M. Volpe, R. Touroude, J. Catal. 242 (2006) 153–161.
[20] J. Scholten, A. Pijpers, M. Hustings, Catal. Rev. Sci. Eng. 27 (1985) 151–206.
[21] A. Dandekar, R. Baker, M. Vannice, J. Catal. 184 (1999) 421–439.
[22] S. Pereda, S. Bottini, E. Brignole, Appl. Catal. A: Gen. 281 (2005) 129–137.
[23] M. Vannice, Kinetics of Catalytic Reactions, Springer Science + Business Media, New York, 2005, pp. 63.
[24] S. Dahl, M.L. Michelsen, AIChE J. 36 (1990) 1829–1836.
[25] C. Binet, A. Jadi, J-C. Lavalley, J. Chem. Soc. Faraday Trans. 88 (1992) 2079–2084.
[26] A. Yee, S.J. Morrison, H. Idriss, J. Catal. 191 (2000) 30–45.
[27] A. Trovarelli, C. de Leitenburg, M. Boaro, G. Dolcetti, Catal. Today 50 (1999) 353–367.
[28] B. Campo, G. Sartori, C. Petit, M. Volpe, Appl. Catal. A: Gen. 359 (2009) 79–83.
[29] P. Levy, M. Primet, Appl. Catal. 70 (1991) 263–276.
[30] J. Lenz, B. Campo, M. Alvarez, M. Volpe, J. Catal. 267 (2009) 50–56.
[31] O. Pozdnyakova, D. Teschner, A. Wootsch, J. Kröhnert, B. Steinhauer, H. Sauer, L. Toth, F.C. Jentoft, A. Knop-Gericke, Z. Paál, R. Schlögl, J. Catal. 237 (2006) 1–16.
[32] D. Tibiletti, E. de Graaf, S. Pheng Teh, G. Rothenberg, D. Farrusseng, C. Mirodatos, J. Catal. 225 (2004) 489–497.
[33] X. Meng, H. Cheng, S. Fujita, Y. Hao, Y. Shang, Y. Yu, S. Cai, F. Zhao, M. Arai, J. Catal. 269 (2010) 131–139.
[34] B. Poling, J. Prausnitz, J. O'Connell, The Properties of Gases and Liquids, McGraw-Hill, New York, 2001, p. 9.71.
[35] J. Kauffman, J. Phys. Chem. A 105 (2001) 3433–3442.
[36] P. Raveedran, S. Wallen, J. Am. Chem. Soc. 124 (2002) 12590–12599.
[37] J. Wang, M. Wang, J. Hao, S. Fujita, M. Arai, Z. Wu, F. Zhao, J. Supercrit. Fluids 54 (2010) 9–15.
[38] A.A. Davydov, Infrared Spectroscopy of Adsorbed Species on the Surface of Transition Metal Oxides, first ed., John Wiley & Sons, London, 1990.